Fit formulas for the angular dependence of the sticking coefficient of energetic hydrocarbon molecules

K. Tichmann, U. von Toussaint, and W. Jacob
Max-Planck-Institut für Plasmaphysik, EURATOM Association, Boltzmannstraße 2, 85748 Garching, Germany

The angular dependence of the sticking coefficient of CH_x projectiles on a prototypical amorphous hydrocarbon surface was studied using molecular dynamics. The resulting datasets are fitted to appropriate fit formulas to allow interpolation and lookup of sticking coefficients at arbitrary parameter values.

I. INTRODUCTION

The amount of tritium that will be retained in wall materials and redeposited layers can possibly limit the operation time of ITER before reaching a security limit[1]. Carbon eroded from the strike point tiles of the divertor will redeposit elsewhere in the machine, codepositing tritium. Making certain assumptions on particle transport and particle-surface interactions, transport simulations calculate how much eroded material will be deposited and where in the machine it will be deposited[2, 3]. Some of the key input parameters for transport codes that include surface effects are sticking and reflection coefficients of hydrocarbon species.

Experimental data for these parameters are scarce. It is known that stable species do not form layers at thermal energies. The sticking coefficient of thermal CH_3 radicals on a–C:H surfaces was determined to be 10^{-4} [4]. Wang et al. [5] investigated the sticking of CH_x^+ ions ($x = 2, 3, 4$) as fraction of ion energy in the energy range from 150 eV to 3000 eV, and found a decrease of the sticking coefficient with increasing number of hydrogen atoms in the molecular ion. All these experiments were performed with the projectiles impinging perpendicular to the surface. Similar MD studies were done for 45° [6, 7] and 60° [7] impact angle. In fusion experiments, charged particles are guided by the magnetic field, so shallow angles for the impinging species are common. To relate the experimental values at perpendicular incidence to the sticking coefficients at arbitrary angles, the sticking coefficient's functional dependence on the angle of incidence is required. Molecular dynamics (MD) offers a straightforward method to study particle-surface interactions on the atomic level. Since in many cases MD simulations are much easier to perform than experiments, they can be used to interpolate between experimental data and to provide information not accessible in the experiment. From MD a sufficient amount of detailed data can be extracted to determine a functional dependence of the sticking coefficient on the angle of incidence. Such parameterised functional dependences are potentially very useful tools for application in plasma boundary transport codes such as EDDY[2] and ERO [3].

II. SIMULATION PROCEDURE

The impact of hydrocarbon ions on an amorphous hydrocarbon surface was simulated using the HCPARCAS code [8] utilising its implementation of the brenner-beardmore hydrocarbon potential. All simulations were performed independent of each other with only one impact per simulation and randomised starting conditions. By this non-cumulative bombardment, a low flux to the sample is simulated. The sample utilised here is composed of 592 carbon and 394 hydrogen atoms. It is 14Å×14Å wide and 28 Å deep with periodic boundary conditions parallel to the surface. It resembles in its parameters (pair-correlation, C/H ratio, sp^2/sp^3 ratio) experimental values of a–C:H samples bombarded with hydrogen atoms with hydrogen fluxes of 10^{18} $m^{-2}s^{-1}$ [9]. The sample creation is presented in more detail in[10, 11]. Due to the moderate flux extreme surface modifications as observed in [12–14] for fluxes partially exceeding 10^{29} $m^{-2}s^{-1}$ can be excluded. However, for fluxes in the range of 10^{25} $m^{-2}s^{-1}$ hydrogen supersaturation[15] may affect the surface properties. The sample temperature was held at 300 K during the simulation. At the beginning of each simulation, the projectile is placed 4 Å above the sample surface with a random position along the surface. The orientation of the projectile was randomised to average over orientation dependent effects found at very low energies [11]. The velocity components of the projectile were set according to the selected projectile energy and angle. Monoenergetic projectiles without internal vibrational or rotational excitations have been used. Additional energy of the internal degrees of freedom may affect sticking and sputtering, especially if the energy stored in internal degrees of freedom is comparable to the kinetic energy of the projectile(see [16] for an MD study using vibrationally hot D_2 projectiles). However, a noticeable contribution is only to be expected for low impact energies. Another point to be kept in mind is that a projectile impact can excite a travelling wave through the sample that can be reflected at the bottom of a finite sized sample. By analysing the velocity components of the atoms as function of the z-coordinate, the incoming wave can indeed be detected for higher impact energies, but the amplitude of the reflected wave was in all instances hidden within the thermal fluctuations. Therefore, an effect of the finite sample size on the results of the simulation is not to be expected. The simulation ran for 40000 time steps, corresponding

to about 10 ps of simulated time. Angles are measured relative to the surface normal.

III. ANALYSIS

For atomic projectiles, the definition of the sticking coefficient is simple: The mean number of projectiles that stick to the surface. For molecular projectiles, this method has to be revised, since the projectile can break up at the surface. If only parts of the molecule stick, the above definition cannot be applied any more. To derive a quantity that is comparable to experiments, where layer thicknesses are measured, the change in the number of carbon atoms, which can be directly correlated to the layer thickness, is used as definition for the molecular sticking coefficient. Furthermore, the MD simulations enable us to distinguish sample and projectile atoms (even if they are indistinguishable in reality). This allows to separate two processes that take place simultaneously: the gross sticking of the projectile and the sputtering of sample material. The sum of these two yields, the *net sticking coefficient*, is the quantity that can be compared to experimental results.

The immediate results from the molecular dynamics calculations are the positions and velocities of all atoms in the simulation. To obtain meaningful macroscopic quantities from this, a large number of simulation runs is required. For each parameter set, 1000 simulations runs were performed. This large number demands an automated analysis that decides whether a given atom is considered stuck or not. This was implemented by determining the distances of the atoms from each other. All atoms with a distance below 2 Å were considered bound to each other, resulting in a network of bound atoms. Disjoint network parts form molecules that are not bound to each other. Every atom that belongs to a molecule above the surface that is not bound to the original sample is considered reflected or sputtered (depending on its origin).

To allow a relatively simple use of the data, the MD results are fitted with appropriate fit formulas. For the sputter yield of monoatomic beams, Eckstein [17] has established a fit formula for the angular dependence:

$$\begin{aligned} Y(E_0,\theta_0) =& Y(E_0,0)\left\{\cos\left[\left(\frac{\theta_0}{\theta_0^*}\frac{\pi}{2}\right)^c\right]\right\}^{-f} \times \\ & \exp\left(b\left\{1-1/\cos\left[\left(\frac{\theta_0}{\theta_0^*}\frac{\pi}{2}\right)^c\right]\right\}\right) \end{aligned} \tag{1}$$

with

$$\theta_0^* = \pi - \arccos\sqrt{\frac{1}{1+E_0/E_{\mathrm{sp}}}}.$$

Angles must be given in radians for these formulas. The parameter E_{sp} is the surface binding energy of the material. The best value for the surface binding energy of a–C:H was determined to be 2.8 eV [18].

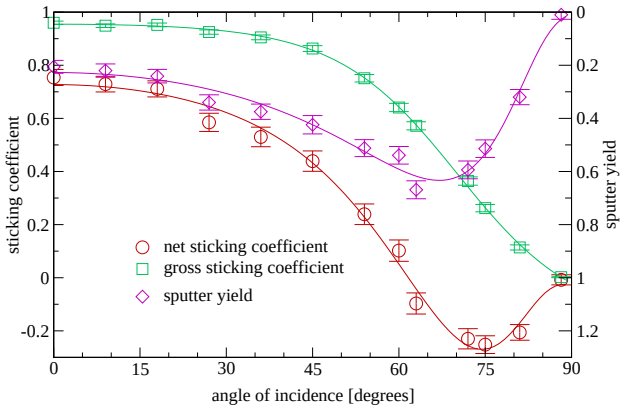

FIG. 1: Gross and net sticking coefficient and sputter yield for CH_3 at 100 eV. The lines are given by formulas (1) and (2)

A fit formula for the gross sticking coefficient was already presented in [19]:

$$S(\alpha) = a_1 \cdot \tanh(a_2 \cdot \cos(a_3\alpha)) + a_4. \tag{2}$$

The parameters a_1 and a_4 of this formula are strongly anti-correlated. To prevent the fitting algorithm from using huge values in these parameters without a noticeable difference in the final χ^2 value, a penalty term was added that restricts the parameter a_4 to ± 0.5.

There is not real physics behind these formulas, but they can be used to interpolate and look up the data. The net sticking coefficient can be calculated form these two fit formulas as

$$S_{\mathrm{net}} = S_{\mathrm{gross}} - Y$$

IV. RESULTS

The sticking of CH_x species was calculated for $x = 0 \ldots 4$ in the energy range from 20 eV to 100 eV and angles of incidence between 0° and 90°. Figure 1 shows the angular dependence of the gross and net sticking coefficient and the sputter yield for 100 eV CH_3. Notice that the sputter yield is plotted inversely on the right hand axis. The principal angular dependence is similar for all investigated species and energies. The gross sticking has a broad maximum around perpendicular incidence and approaches zero for grazing incidence. The sputtering is relatively low at perpendicular incidence and raises to a maximum between 60° and 70°. At large angles of incidence (i.e. close to 90°), the sputter yields rapidly approaches zero. The resulting net sticking coefficient thus starts at a high value at perpendicular incidence and goes down to a minimum with net erosion near 75° for datasets with sufficiently high energy. At grazing incidence, the net sticking coefficient goes back to zero. The solid lines in figure 1 are fits to the data according to fit formulas

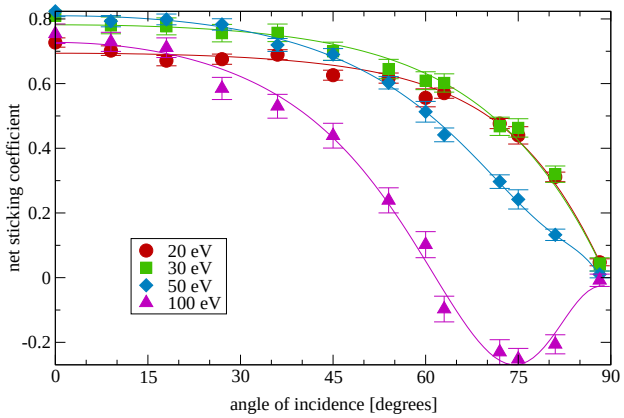

FIG. 2: Net sticking coefficient of CH_3 for different incident energies as a function of angle of incidence. The lines are fits to the MD data (see text).

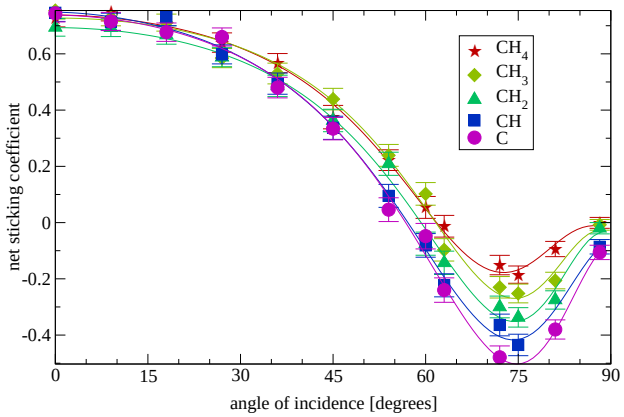

FIG. 3: Angular dependence of the net sticking coefficient at 100 eV projectile energy for different projectiles

(1) and (2). The resulting fit parameters are compiled in tables I and II.

Figure 2 shows the angular dependence of the net sticking coefficient of CH_3 for different projectile energies. For the lower energies, there is always net deposition and the two curves at 20 eV and 30 eV show almost identical behaviour. At 50 eV, the net sticking coefficient decreases for larger angles faster than the data for 20 eV and 30 eV. This is due to the increasing importance of sputtering. At 100 eV incident energy, the sputter yield exceeds the gross sticking coefficient for angles lager than 60°, leading to net erosion between 60° and 90°. A detailed analysis of the energy dependence at perpendicular incidence is given in [20].

The angular dependence of the net sticking coefficient is approximately similar for different choices of projectile species. The results for a selection of species are shown in figure 3. All plots in figure 3 are for 100 eV projectile energy. They all show a net erosion range at large angles. However, while the stable CH_4 erodes only up to 0.2 carbon atoms per impact, the radical projectile species with less hydrogen atoms erode successively more with CH eroding up to 0.4 carbon atoms per impact. The angle where the erosion yield is at its peak slightly shifts from CH_4 to the radical species, but given that there are only two data points in this region, this is probably insignificant. At perpendicular incidence, all projectiles behave very similar. Only for CH_2, the net sticking coefficient is significantly lower at small angles up to 30°, all other projectile species show no differences in this range.

	E_0[eV]	$Y(0)$	E_{sp}[eV]	f	b	c
CH_4	20	0.00152	2.8	20.1	14.8	0.492
	30	0.0306	2.8	-2.76	-0.447	1.13
	50	0.0799	2.8	3.19	1.84	1.23
	100	0.213	2.8	6.36	3.46	0.914
CH_3	20	0.0118	2.8	8.7	5.72	0.957
	30	0.0433	2.8	3.71	2.34	1.07
	50	0.106	2.8	3.09	1.44	1.19
	100	0.227	2.8	5.1	2.51	0.966
CH_2	20	0.0316	2.8	7.08	4.4	1.1
	30	0.0879	2.8	1.66	0.852	1.35
	50	0.145	2.8	3.46	1.63	1.13
	100	0.264	2.8	4.9	2.37	0.96
CH	10	0.0143	2.8	7.36	4.71	1.52
	20	0.0566	2.8	3.91	2.22	1.17
	50	0.129	2.8	5.23	2.53	0.966
	100	0.221	2.8	6.5	3.19	0.841
C	10	0.0105	2.8	7.75	4.4	2.17
	20	0.0501	2.8	2.96	1.62	1.28
	50	0.139	2.8	3.99	1.76	1.08
	100	0.236	2.8	5.9	2.76	0.886

TABLE I: Parameters for the sputter yield fit formula (1).

V. CONCLUSIONS

Using molecular dynamics, a large database of sticking coefficients of different hydrocarbon projectiles was computed. The energy of the projectile ranged from 20 eV to 100 eV and the angle of incidence was varied from perpendicular incidence to 88°. To compress and interpolate the data, analytical formulas (1) and (2) were fitted to the MD data. The corresponding fit coefficients are compiled in tables I and II.

At sufficiently high energies, erosion dominates the surface processes for angles of incidence larger than 60°. For smaller angles, the behaviour is nearly independent on the projectile species.

	E_0[eV]	a_1	a_2	a_3	a_4
CH_4	10	-1.31	-0.00767	1.87	0.00936
	20	0.28	0.868	1.01	-0.004
	30	0.285	1.32	1.49	0.323
	50	0.645	1.82	1.17	0.259
	100	0.55	2.1	1.34	0.417
CH_3	10	1.1	3.19	0.902	-0.503
	20	1.25	2.69	0.897	-0.537
	30	1.39	2.38	0.895	-0.539
	50	1.48	1.94	0.896	-0.503
	100	0.583	2.05	1.28	0.39
CH_2	10	1.4	3.2	0.905	-0.53
	20	1.44	2.95	0.901	-0.542
	30	1.45	2.59	0.89	-0.547
	50	1.51	1.93	0.881	-0.53
	100	0.611	1.98	1.25	0.369
CH	10	1.45	2.58	0.836	-0.518
	20	1.46	2.54	0.846	-0.517
	50	1.48	1.82	0.882	-0.449
	100	0.617	1.9	1.25	0.38
C	10	1.44	2.58	0.854	-0.516
	20	1.49	2.59	0.85	-0.534
	50	1.53	2.07	0.896	-0.512
	100	0.646	1.89	1.22	0.357

TABLE II: Parameters for the gross sticking coefficient fit formula (2)

[1] J. Roth, E. Tsitrone, A. Loarte, Th. Loarer, G. Counsell, R. Neu, V. Philipps, S. Brezinsek, M. Lehnen, P. Coad, Ch. Grisolia, K. Schmid, K. Krieger, A. Kallenbach, B. Lipschultz, R. Doerner, R. Causey, V. Alimov, W. Shu, O. Ogorodnikova, A. Kirschner, G. Federici, A. Kukushkin, EFDA PWI Task Force, ITER PWI Team, Fusion for Energy, and ITPA SOL/DIV. Recent analysis of key plasma wall interactions issues for ITER. *J. Nucl. Mater.*, 390–391:1–9, 2009.

[2] K. Ohya and A. Kirschner. Modeling of erosion and deposition by the Monte Carlo codes EDDY and ERO. *Phys. Scripta*, T138:014010 (7pp), 2009.

[3] A. Kirschner, K. Ohya, D. Borodin, R. Ding, D. Matveev, V. Philipps, and U. Samm. Prediction of long-term tritium retention in the divertor of ITER: influence of modelling assumptions on retention rates. *Phys. Scripta*, T138:014011 (6pp), 2009.

[4] A. von Keudell, T. Schwarz-Selinger, M. Meier, and W. Jacob. Direct identification of the synergism between methyl radicals and atomic hydrogen during growth of amorphous hydrogenated carbon films. *Applied Physics Letters*, 76(6):676–678, 2000.

[5] Wenmin Wang, J. Roth, W. Eckstein, R. Schwoerer, H. Plank, and Maohua Du. Deposition of amorphous hydrogenated carbon films due to hydrocarbon molecule ion-beam bombardment. *Nuclear Instruments and Methods in Physics Research Section B: Beam Interactions with Materials and Atoms*, 129(2):210 – 216, 1997.

[6] K. Ohya, Y. Kikuhara, K. Inai, A. Kirschner, D. Borodin, A. Ito, H. Nakamura, and T. Tanabe. Simulation of hydrocarbon reflection from carbon and tungsten surfaces and its impact on codeposition patterns on plasma facing components. *Journal of Nuclear Materials*, 390-391:72 – 75, 2009. Proceedings of the 18th International Conference on Plasma-Surface Interactions in Controlled Fusion Devices.

[7] D A Alman and D N Ruzic. Molecular dynamics simulation of hydrocarbon reflection and dissociation coefficients from fusion-relevant carbon surfaces. *Physica Scripta*, 2004(T111):145, 2004.

[8] K. Nordlund, J. Keinonen, and T. Mattila. Formation of ion irradiation induced small-scale defects on graphite surfaces. *Phys. Rev. Lett.*, 77(4):699–702, Jul 1996.

[9] T. Schwarz-Selinger, A. von Keudell, and W. Jacob. Plasma chemical vapor deposition of hydrocarbon films: The influence of hydrocarbon source gas on the film properties. *J. Appl. Phys.*, 86:3988, 1999.

[10] P. N. Maya, U. von Toussaint, and C. Hopf. Synergistic erosion process of hydrocarbon films: A molecular dynamics study. *New J. Phys.*, 10:023002 (15pp), 2008.

[11] A.R. Sharma, R. Schneider, U. Toussaint, and K. Nordlund. Hydrocarbon radicals interaction with amorphous carbon surfaces. *Journal of Nuclear Materials*, 363-365:1283 – 1288, 2007. Plasma-Surface Interactions-17.

[12] P. S. Krstić, C. O. Reinhold, and S. J. Stuart. Chemical sputtering from amorphous carbon under bombardment by deuterium atoms and molecules. *New J. Phys.*, 9:209 (1–25), 2007.

[13] P. S. Krstic, C. O. Reinhold, and S. J. Stuart. Energy and angle spectra of sputtered particles for low-energy deuterium impact of deuterated amorphous carbon. *Journal of Applied Physics*, 104(10):103308, 2008.

[14] E.D. de Rooij, U. von Toussaint, A.W. Kleyn, , and W.J. Goedheer:. Molecular dynamics simulations of amorphous hydrogenated carbon under high hydrogen fluxes. *Phys. Chem. Chem. Phys.*, 11:9823–9830, 2009.

[15] E. Salonen, K. Nordlund, J. Tarus, T. Ahlgren, J. Keinonen, and C.H. Wu. Suppression of carbon erosion by hydrogen shielding during high-flux hydrogen bombardment. *Phys. Rev. B*, 60:R14005–1–4, 1999.

[16] P. S. Krstić, C. O. Reinhold, and S. J. Stuart. Chemical sputtering by impact of excited molecules. *Europhys. Lett.*, 77:33002 p1–p6, 2007.

[17] Wolfgang Eckstein. Sputtering yields. *Sputtering by Particle Bombardment*, pages 33–187, 2007.

[18] W. Jacob, C. Hopf, and M. Schlüter. Chemical sputtering of carbon materials due to combined bombardment by ions and atomic hydrogen. *Phys. Scripta*, T124:32–36, 2006.

[19] K Tichmann, U von Toussaint, T Schwarz-Selinger, and W Jacob. Determination of the sticking probability of hydrocarbons on an amorphous hydrocarbon surface. *Physica Scripta*, 2009(T138):014015, 2009.

[20] K. Tichmann, U. von Toussaint, and W. Jacob. Investigating the sticking of low energy hydrocarbons using molecular dynamics. *New J. Phys.*, submitted.